Identification of the Zn(II) Site in the Copper-Responsive Yeast Transcription Factor, AMT1: A Conserved Zn Module†

Rohan A. Farrell, Joanne L. Thorvaldsen, and Dennis R. Winge*

University of Utah Health Sciences Center, Salt Lake City, Utah 84132

Received July 24, 1995; Revised Manuscript Received October 4, 1995⊗

ABSTRACT: The N-terminal metal-binding domains of the copper-activated yeast transcription factors, ACE1 and AMT1, bind to specific DNA sequences in a Cu-dependent fashion. Recombinant AMT1 and ACE1 metal-binding domains are isolated as Cu_4Zn_1−protein complexes. Site-directed mutagenesis of AMT1 was used in this study to map the ligands of the Cu(I) and Zn(II) ions. The results are consistent with the N-terminal halves of AMT1 and ACE1 consisting of two independent submodules, one binding a single Zn(II) ion and the second binding the tetracopper cluster. The basis of this conclusion is, first, that mutations of two cysteinyl codons and a histidyl codon in the first 42 residues of AMT1 do not alter DNA binding. In contrast, serine substitutions at four cysteine positions at codons 43, 61, 90, and 98 abolish DNA binding. We demonstrated previously that population of the Zn(II) site in AMT1 does not alter the ability of the protein to bind DNA but bound Cu(I) ions are essential for DNA binding [Thorvaldsen, J. L., et al. (1994) *Biochemistry 33,* 9566−9577]. Second, mutations in the N-terminal 42 residue segment reduce the Zn(II) content of purified mutant AMT1 molecules. Third, a synthetic peptide consisting of the N-terminal 42 residues in AMT1 forms a stable Zn(II) complex and substitution with Co(II) reveals an electonic spectrum identical to that of the Co-substituted intact Cu_4AMT1 protein. ^{113}Cd(II) NMR studies reveal that the divalent metal site consists of ligands provided by three cysteinyl thiolates and a single histydyl imidazole. The sequence homology between AMT1, ACE1, and MAC1 in the N-terminal 42 residues suggests that ACE1 and MAC1 will, likewise, contain N-terminal Zn modules. A 42-residue ACE1 synthetic peptide gives identical metal binding properties to the corresponding AMT1 synthetic peptide. Thus, AMT1 and likely ACE1 consist of two contiguous modules, residues 1−42 forming an independent Zn(II) module and residues 43−110 enfolding a tetracopper cluster.

Yeast cells require copper ions for a variety of enzyme functions including cytoplasmic superoxide dismutase (SOD) and cytochrome oxidase. Most yeast strains can proliferate in culture medium containing copper salts in excess of 0.1 mM. Laboratory strains able to grow in medium containing in excess of 0.3 mM Cu(II) are designated copper resistant. One major discriminating factor between copper sensitive and copper resistant cells is the metallothionein (MT) locus (Karin et al., 1984; Fogel et al., 1983). Copper resistant strains of *Saccharomyces cerevisiae* and *Candida glabrata* contain tandemly amplified MT genes (Fogel & Welch, 1982; Mehra et al., 1990). Targeted disruption of the *CUP1* MT genes in *S. cerevisiae* and *MTII* genes in *C. glabrata* leads to a copper hypersensitive phenotype (Hamer et al., 1985; Ecker et al., 1986; Mehra et al., 1992). MT confers copper resistance in yeast by buffering the intracellular Cu(I) concentration. Cu(I) ions bind to the *S. cerevisiae* MT within a single Cu_7S_{10} complex with cysteinyl thiolate ligands (Narula et al., 1991).

The synthesis of MT is coupled to the intracellular copper concentration in yeast through Cu-induced transcriptional activation of MT gene expression (Thiele & Hamer, 1986; Furst et al., 1988). The response of MT transcriptional activation is restricted to copper stress in yeast (Hamer, 1986; Furst et al., 1988). Ag(I) is the only other metal ion known to induce limited MT expression in *S. cerevisiae* and *C. glabrata*. Induction by both Cu(I) and Ag(I) is expected as these ions exhibit similar coordination properties (Dance, 1978). The metal ion specificity for the induction of MT genes in yeast is in contrast to mammalian cells in which multiple metal ions mediate MT induction (Hamer, 1986; Palmiter, 1987).

The *trans*-acting factors mediating Cu-dependent regulation of MT genes in *S. cerevisiae* and *C. glabrata* are designated ACE1 (or CUP2) and AMT1, respectively (Thiele, 1988; Welch et al., 1989; Zhou & Thiele, 1991; Zhou et al., 1992). The 225-residue ACE1 polypeptide appears to consist of two segments with distinct functions (Furst et al., 1988). The binding of ACE1 to *CUP1* MT promoter sequences maps to the N-terminal half of ACE1 and this segment of the polypeptide contains multiple cysteinyl residues in Cys-x-Cys or Cys-x-x-Cys sequence motifs (Furst et al., 1988; Buchman et al., 1989). Eleven cysteinyl residues are critical for the ACE1 function of Cu-induced expression of *CUP1* (Hu et al., 1990). The C-terminal segment of ACE1 is similar to many fungal transcription factors in the abundance of acidic residues and is believed to be the transactivation domain. This domain is critical for Cu-induced *CUP1* expression (Thiele, 1988).

Cu-induced expression of the three MT genes in *C. glabrata* is mediated by AMT1 (Zhou & Thiele, 1991; Zhou et al., 1992). AMT1 is 50% homologous to ACE1 of *S. cerevisiae* in the DNA-binding N-terminal segment of the

† This work was made possible by Grant ES 03817 from the National Institute of Environmental Health Sciences, NIH, to D.R.W.

* To whom correspondence should be addressed. Fax: 801-585-5469. E-mail: dennis.winge@hsc.utah.edu.

⊗ Abstract published in *Advance ACS Abstracts,* January 15, 1996.

0006-2960/96/0435-1571$12.00/0

polypeptide (Zhou & Thiele, 1991). The eleven critical ACE1 cysteinyl residues are conserved in AMT1. ACE1 and AMT1 binding sites within the 5′ flanking sequences of MT genes in the two yeasts are related in sequence with a conserved tetranucleotide core region (Zhou et al., 1992). AMT1 can functionally replace ACE1 in *S. cerevisiae* and confer Cu-induced expression on *CUP1* (Thorvaldsen et al., 1993).

The mechanism of Cu-induced expression of yeast MT genes lies in the Cu activation of ACE1 and AMT1. The activation process involves formation of a polycopper cluster with cysteinyl thiolates as ligands (Dameron et al., 1991; Nakagawa et al., 1991; Thorvaldsen et al., 1994). In biophysical studies carried out on the N-terminal segments of ACE1 and AMT1 molecules expressed in bacteria, we demonstrated that AMT1 was purified as a Cu,Zn-protein from bacterial cultures grown in the presence of $CuSO_4$ (Thorvaldsen et al., 1994). Chemical analysis revealed 4 and 1 mol equiv of copper and zinc ions bound, respectively (Thorvaldsen et al., 1994). Electrospray mass spectrometry was used to verify that a uniform species was present with 4 Cu(I) ions and 1 Zn(II) ion bound per AMT1 molecule (Thorvaldsen et al., 1994). Binding of the 4 Cu(I) ions in AMT1 occurs in an all-or-nothing process and the observation of a 2.7 Å Cu−Cu scatter interaction by EXAFS in both AMT1 and ACE1 is consistent with a polycopper cluster (Dameron et al., 1991; Nakagawa et al., 1991; Thorvaldsen et al., 1994). A series of tetracopper thiolate clusters have been structurally characterized with small thiolate ligands (Dance, 1986). On the basis of EXAFS of CuACE1, CuAMT1, and synthetic $[Cu_4(SPh)_6]^-$ complexes, it appears that the Cu(I) ions in ACE1 and AMT1 exhibit trigonal coordination (Thorvaldsen et al., 1994; Pickering et al., 1993).

The observation of Zn(II) in bacterially expressed AMT1 raises the question of whether AMT1 in yeast would, likewise, contain bound Zn(II). A number of observations suggest that AMT1 may indeed contain Zn(II) in yeast. First, AMT1 is invariably isolated with one bound Zn(II) ion from bacteria cultured in the presence of 1000 μM $CuSO_4$ (the medium Zn concentration is 2 μM). Second, Cu(I) reconstitution studies of AMT1 did not reveal Cu(I) ions bound in excess of 4 mol equiv. This is in contrast to ACE1 in which *in vitro* Cu(I) reconstitution studies showed maximal binding of 6 mol equiv of Cu(I) (Dameron et al., 1991). It is likely that exogenous Cu(I) can displace the bound Zn(II) ion in ACE1, whereas this displacement does not occur in AMT1. These results are suggestive but do not prove that the metal content of bacterially isolated AMT1 is the physiological metal ion content. Further studies to support the physiological presence of Zn(II) in AMT1 and ACE1 in yeast are presented in this report.

The Cu_4Zn_1 complex of AMT1 may consist of a tetracopper cage cluster and a distinct Zn(II) site. The ability of AMT1 to bind DNA was shown to be dependent on population of the Cu(I) sites but not the Zn(II) site (Thorvaldsen et al., 1994). Formation of the polycopper center in AMT1 stabilizes a tertiary fold that is competent to bind DNA (Thorvaldsen et al., 1994).

Limited information exists on the DNA binding sites for AMT1, yet multiple analyses of the ACE1 DNA binding sites have been reported (Buchman et al., 1990; Dobi et al., 1995). The interaction of ACE1 with its DNA binding site spans one and a half turns of a B-form DNA helix (Buchman et al. 1990). ACE1 makes base specific contacts within the major groove at the two ends of the UAS sequence and makes contacts within the minor groove near the middle of the UAS element (Buchman et al., 1990; Dobi et al., 1995). If the AMT1−DNA complex resembles the ACE1−DNA complex, it is conceivable that the tetracopper center and Zn(II) organize separate domains for protein−DNA contact.

In this report we demonstrate that bacterially expressed ACE1 is also isolated as a stable Cu_4Zn_1 complex. Mutagenesis was used to identify three cysteinyl residues nearest the N-terminus in AMT1 as Zn(II) ligands. A synthetic peptide of 42 amino acids corresponding to residues 1−42 mimicked the properties of the Zn(II) site in the intact AMT1 molecule and revealed that the Zn(II) site ligands consist of three cysteinyl residues and a single histidine. The results suggest that the DNA-binding domain of AMT1 (residues 1−110) consists of two subdomains: residues 1−42 forming the Zn(II) module and residues 43−110 enfolding the candidate tetracopper center.

MATERIALS AND METHODS

Mutagenesis. An *Eco*RI/*Bam*HI fragment containing the AMT1 synthetic gene was cloned into pBluescript (Stratagene) to make vector pBS-ABC (Thorvaldsen et al., 1994). The gene was removed as a *Hin*dIII/*Sac*I fragment and cloned into vector pAlter (Promega) to create vector pAltAMT which was subsequently used in site directed mutagenesis by previously described methodology (Sewell et al., 1995). Mutant AMT1 genes were removed as an *Nco*I/*Bam*HI fragment and cloned into vector pET9d (Novagen) for expression. The predicted mutations were confirmed by DNA sequencing of the AMT1 gene using Sequenase (U.S. Biochemicals) and electrospray mass spectrometry of the mutant proteins.

The *ACE1* gene was subcloned from pHAC (Thorvaldsen et al., 1993) as a 1.7 kb *Hin*dIII/*Sac*I fragment. The fragment was subcloned into pAlter-1 (Promega). Mutations were generated as described previously (Sewell et al., 1995). Mutations were confirmed by nucleotide sequencing. The confirmed mutations were subcloned as *Hin*dIII/*Sac*I fragments into both YEp352 and YCplac33. Plasmids were transformed into DTY23 yeast cells and selected on synthetic complete medium lacking uracil. Standard yeast culturing methods were used.

Protein Purification. Mutant AMT1 molecules and wild-type ACE1 were purified as described previously (Thorvaldsen et al., 1994). ACE1 was expressed as a 141 residue polypeptide from a pET3d expression plasmid as described previously (Dameron et al., 1991). Mutant AMT1 and ACE1 molecules were expressed in *Escherichia coli* BL21 (pLysS) cells after induction with 0.4 mM isopropyl β-D-thioglactopyranoside (IPTG) of cells at OD_{600nm} 0.5. Following a 30 min induction $CuSO_4$ was added to a final concentration of 1 mM. The Zn(II) concentration in the medium was 2 μM. After a 3 h incubation, cells were harvested by centrifugation and washed in 0.25 M sucrose. The final cell pellet was resuspended in lysis buffer (10 mM sodium phosphate, 0.1 M KCl, 0.1% β-mercaptoethanol, pH 7.8) and stored at −70 °C. Thawed cells were disrupted by sonication and the extract was clarified. Remaining AMT1 protein in the pellet fraction was further extracted by sonication in the presence

of 5 mg/mL protamine sulfate and centrifuged. The initial supernatant and the protamine-extracted supernatant were pooled and further extracted with protamine (1 mg of protamine per 5 mg of total protein).

AMT1 and ACE1 proteins were purified from cell extracts by carboxymethyl-cellulose chromatography. All buffers contained 4 mM DTT to minimize adventitiously bound copper ions and to keep copper ions reduced. The proteins were eluted with a linear gradient of 0.1−0.4 M KCl in 10 mM sodium phosphate and 4 mM DTT, pH 7.8. AMT1- and ACE1-containing fractions were pooled and concentrated by YM3 ultrafiltration. The sample was equilibrated in 50 mM HEPES and 4 mM DTT, pH 7.8, and subsequently chromatographed on MonoS (Pharmacia-LKB) using a linear gradient from 0 to 0.75 M KCl in the equilibration buffer. Spectral measurements were made on mutant proteins immediately after purification as slow, apparent autolysis occurs in AMT1 samples upon storage. This autolysis results in cleavage of a limited number of peptide bonds in AMT1 in both the Zn and Cu modules (data not shown). The cleavage results in reduced DNA affinity, but not diminished metal content. To avoid problems arising from this time-dependent peptide bond cleavage, extracts were used as source of mutant AMT1 proteins for gel shift analyses rather than purified proteins.

Peptide Synthesis. Peptides corresponding to the N-terminal 42 residues of AMT1 and ACE1 were synthesized by standard Fmoc chemistry on an ABI 431A instrument. Only one predominant product was recovered after cleavage of each peptide and purification was accomplished by C_{18} reverse-phase HPLC on preparative and semipreparative columns. AMT1-42 and ACE1-42 peptides eluted at 35% and 38% acetonitrile, respectively, on C_{18} reverse phase HPLC. Electrospray MS of the purified peptide was used to verify the correctness of the sequence. The peptide was quantified by amino acid analysis and thiol titrations with dithiodipyridine.

Chemical Analyses. Metal analysis was performed on a Perkin-Elmer 305A spectrometer. Protein was quantified by amino acid analysis after hydrolysis in 5.7 N HCl containing 0.1% phenol *in vacuo* at 110 °C with analysis performed on a Beckman 6300 analyzer.

Electrospray mass spectrometry was performed on a Fisons Instruments Trio 2000 mass spectrometer (VG Biotech., Cheshire U.K.) under the following conditions: probe potential, 2.3 kV; counter electrode potential, 0.25 kV; and sampling cone potential, 46 V. The instrument was scanned from *m/z* 700 to 1700 at a rate of 10 s per scan, and 10−25 scans were summed to obtain each spectrum. The AMT1 samples were analyzed in 10 mM Tris-HCl, pH 7, or in samples diluted to 1% glacial acetic acid. The solutions were infused into the mass spectrometer at a rate of 4−6 μL/min using a Harvard syringe pump. Other experimental details are described previously (Thorvaldsen et al., 1994).

Zn-free CuAMT1 complexes were prepared by acidification to pH 4 followed by gel filtration on Sephadex G-25 at pH 4. Co(II) reconstitution of Zn-depleted AMT1 was carried out anaerobically by mixing Zn-free CuAMT1 mutant proteins with a predetermined molar equivalency of Co(II) followed by neutralization to pH 7.

Spectroscopy. Optical absorption spectroscopy was carried out on a Beckman DU-65 recording spectrophotometer. Co(II)-containing AMT1 samples were scanned anaerobically. Cu(I) complexes with AMT1 and ACE1 peptides were prepared anaerobically using Cu(I)−acetonitrile, and the samples were monitored for emission. Luminescence measurements were made on a Perkin-Elmer 650-10S fluorimeter with excitation at 300 nm. ^{113}Cd NMR spectroscopy was performed on a Unity 500 Varian spectrometer operating in the Fourier transform mode at 110.89 MHz. Spectra were recorded on a ^{113}Cd sample containing 3 mg of polypeptide and $^{2}H_2O$ as a field lock. The heteronuclear multiple-quantum coherence (HMQC) spectrum was recorded using the standard HMQC pulse sequence with solvent presaturation (Bax et al., 1983; Bax & Subramanian, 1986).

Gel Shift. Gel shift analyses were performed using whole cell extracts from *E. coli* BL21 cells expressing normal and mutant forms of the metal-binding domain of the AMT1 protein. Cells induced with IPTG as described above were harvested, washed with 0.25 M sucrose, and suspended in 10 mM sodium phosphate and 4 mM DTT at pH 7.8 for lysis by sonication. The lysate was subsequently clarified by centrifugation, and the supernatant was quantified for protein by the method of Bradford et al. (1976). Total protein and induction levels of normal and mutant AMT1 proteins were confirmed by SDS gel electrophoresis.

Oligonucleotides spanning the AMT1 binding site of the *AMT1* gene (Thorvaldsen et al., 1994) were synthesized with an ABI 380B DNA synthesizer. The oligonucleotides and gel shift conditions were described previously (Thorvaldsen et al., 1994). The protein:DNA incubations included 0.01% Nonidet P40, 30 μg/mL poly(dI-dC), 65 mM KCl, 10 mM canine albumin, 0.25 mM $MgCl_2$, and 4 mM DTT and 0.5 μg of protein.

RESULTS

We previously reported that purification of the N-terminal 110 residue AMT1 polypeptide from bacteria after expression of a synthetic AMT1 gene resulted in the isolation of a uniform species containing 4 Cu(I) ions and a single Zn(II) ion (Thorvaldsen et al., 1994). The single Zn(II) ion in AMT1 persisted in cultures grown in the presence of 1.4 mM $CuSO_4$ and was not displaced by added Cu(I) *in vitro*. Using the same purification protocol the 122-residue ACE1 polypeptide was also purified as a Cu,Zn-protein. The mean Cu and Zn content of the isolated ACE1 complex was 4.5 mol equiv of Cu(I) and 1.1 mol equiv of Zn(II) (two independent isolates).

As part of our efforts to determine any physiological role of the bound Zn(II) in AMT1 and ACE1, we set out to identify the Zn(II) ligands in AMT1. AMT1 was the preferred target as the expression of the N-terminal half of AMT1 in *E. coli* exceeded that of the N-terminal half of ACE1. Our previous biophysical work on the 110-residue AMT1 fragment indicated that Zn(II) was coordinated by 3−4 sulfur atoms and that the ability of AMT1 to form a specific complex with DNA was independent of occupancy of the Zn(II) site (Thorvaldsen et al., 1994). The strategy was to mutagenize cysteinyl codons in AMT1 to determine whether a particular mutation altered the bound Zn(II) content or affected DNA binding. The codons mutagenized are shown in Figure 1. Ten of the eleven cysteines in the 110-residue AMT1 fragment exist as pairs of cysteinyl residues separated by one or two other residues. Our ligand mapping strategy was to mutate the first cysteinyl codon of each CxC

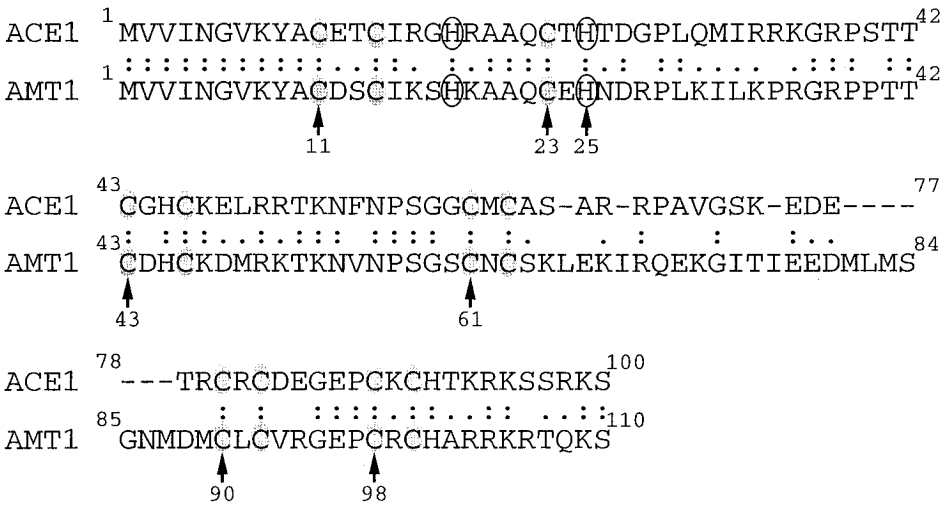

FIGURE 1: Sequence comparison of the N-terminal DNA binding segements of AMT1 and ACE1. Arrows specify the codons mutated in AMT1. The conserved cysteinyl codons are shaded and the two conserved histydyl residues, one of which is the fourth Zn(II) ligand, are encircled.

or CxxC pair. The assumption was that CxC or CxxC sequence motifs in AMT1 would provide pairs of sulfur atoms for ligation of the same metal ion or different metal ions within a single cluster. In the superfamily of Zn module proteins CxC and CxxC pairs typically coordinate the same metal ion (Blake & Summers, 1994), whereas such cysteine pairs can coordinate different metals within a single cluster as in metallothionein (Robbins et al., 1991). A common $Cx_{1-2}C$ structural motif in metal-binding proteins is a half-turn with two sulfur atoms in van der Waals contact and the turn stabilized by a backbone amide→sulfur hydrogen bond (Blake & Summers, 1994).

Cysteinyl codons in AMT1 were mutatated to seryl codons, except Cys11 was mutated to a tyrosine which mimics the original *ace1-1* mutation (Buchman et al., 1989). Besides the CxC pairs, Cys23 and His25 codons were mutated to seryl codons. Mutations were made in the synthetic gene for AMT1 encoding the N-terminal 110 residues. The desired mutations were confirmed by nucleotide sequencing. Mutant *AMT1* genes were cloned into pET vectors for expression in *E. coli*. Each mutant AMT1 molecule was expressed to similar levels as judged by a stained SDS−polyacrylamide electrophoresis gel (Figure 2A).

The first prediction was that mutations in codons of residues important for Zn(II) coordination should not markedly affect DNA binding. Extracts of *E. coli* cells containing pET vectors with mutated AMT1 genes were tested for DNA binding by the gel retardation assay (Figure 2B). A AMT1−DNA complex was observed for C11Y, C23S, and H25S mutants, but not for the C43S, C61S, C90S, and C98S mutants. A faint indication of a complex was observed with C90S. This experiment demonstrates that mutations at codons 43, 61, 90, and 98 result in reduced DNA affinity. No attempt was made to compare the DNA affinity of C11Y, C23S, and H25S molecules with wild-type AMT1.

The second prediction was that mutations in codons of residues important for Zn(II) binding should destabilize Zn(II) binding and may result in reduced Zn(II) binding. Furthermore, mutations in Cu(I) ligand codons may affect formation of tetracopper center but may not alter Zn binding if Zn(II) is bound within a discreet domain. Mutant AMT1 molecules were purified to homogeneity and analyzed for

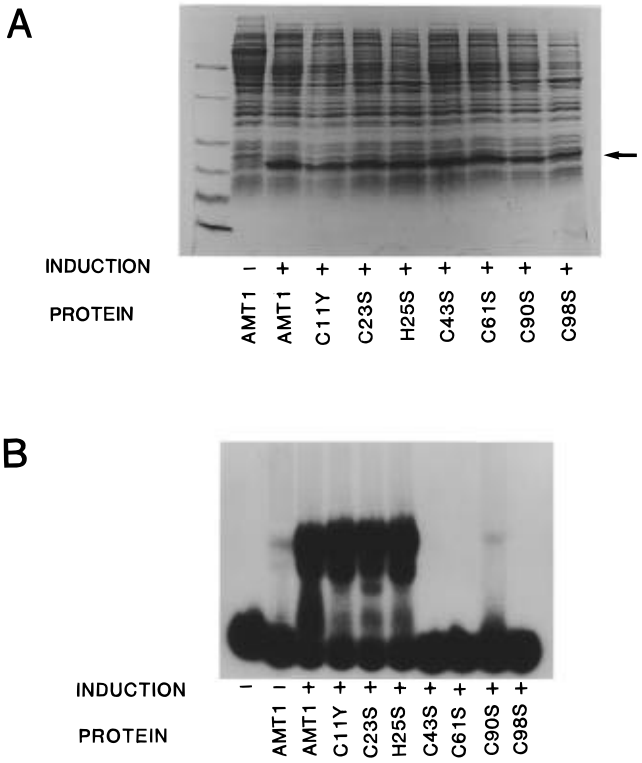

FIGURE 2: Bacterial expression and DNA binding properties of AMT1 mutants. Panel A shows the Comassie stained polypeptides in extracts of *E. coli* expressing wild-type or mutant AMT1 proteins in the presence (+) or absence (−) IPTG induction. The arrow specifies the position of the AMT1 polypeptides. Panel B is gel shift analyses of the same extracts using an AMT1-specific DNA duplex as the radiolabeled probe.

Cu and Zn content (Table 1). Chemical analyses revealed a normal Zn content for all mutants except for low values with C23S and H25S molecules and high Zn levels in the C90S mutant. The copper content was slightly reduced for the C23S and C61S mutants and elevated for the H25S mutant.

Electrospray mass spectrometry was used to verify the metal stoichiometry of the mutant AMT1 complexes (Table 1). Since we cannot discriminate the masses of Zn and Cu by this technique, we can only assess the number of metal ions bound from the mass of the complex. We showed previously that a M5 species was the dominant species at

Table 1: Metal Binding Stoichiometries of Mutant Forms of AMT1

protein	Cu:protein (mol equiv)	Zn:protein (mol equiv)		metallated species by MS at pH 4
wild-type[a]	4.2 ± 0.2	1.2 ± 0.2	(n = 8)	M4
C11Y	4.3 ± 0.4	1.0 ± 0.1	(n = 6)	M4
C23S	3.4 ± 0.4	0.3 ± 0.1	(n = 2)	
H25S	5.5 ± 0.2	0.5 ± 0.1	(n = 4)	
C43S	4.5 ± 0.3	1.2 ± 0.1	(n = 2)	M4
C61S	3.1 ± 0.5	1.0 ± 0.1	(n = 3)	M4
C90S	4.1 ± 0.1	2.5 ± 0.1	(n = 2)	M4
C98S	3.9 ± 0.4	1.25 ± 0.2	(n = 4)	M4

[a] Data of wild-type AMT1 is from Thorvaldsen et al. (1994). The n value specifies the number of independent isolates analyzed and standard deviations are shown.

pH 7, but at pH 4 an M4 species was dominant (Thorvaldsen et al., 1994). Chemical analyses revealed that Zn(II) was dissociated at pH 4 leaving the tetracopper complex intact (Thorvaldsen et al., 1994). Mass spectrometry of the the C11Y protein at pH 7 showed only a M4 species, and this species was also evident at pH 4. At pH 7 the C43S mutant AMT1 complex revealed not only major M5 complexes but also low amounts of a species whose mass was consistent with a M6 complex. For unknown technical reasons we were unable to obtain mass spectrometry data at pH 7 on the remaining mutant proteins. The C→S mutations may alter the protein to impede ionization. However, the M4 complex was the major species observed at pH 4 for C43S, C61S, C90S, and C98S mutant AMT1 molecules. We were unable to obtain mass data for C23S and H25S mutant molecules at pH 4.

The existence of only a M4 species at pH 7 for the C11Y protein may indicate that the single Zn(II) ion bound to C11Y AMT1 may be bound with reduced affinity or in an altered site. To determine whether the C11Y mutation altered the Zn(II) coordination site, the bound Zn(II) in the C11Y mutant AMT1 was replaced with a Co(II) ion to permit electronic spectroscopy of Co(II) complexes. Substitution of Co(II) for the Zn(II) in C11Y revealed a marked blue-shift in the spectrum and loss of the 740 nm transition in the d-d band which is consistent with loss of a sulfur ligand (Figure 3). For comparison, the electronic spectrum of the intact Co_1Cu_4AMT1 complex is shown in Figure 3.

If Zn(II) liganding atoms are provided by Cys11, Cys14, Cys23, and His25 and Cu(I) liganding atoms from the remaining cysteinyl residues, one prediction was that the d-d electronic transition envelope would be unaffected in mutant AMT1 molecules with substitutions in the tetracopper ligands. Substitution of Co(II) for Zn(II) in C61S mutant AMT1 followed by electronic spectroscopy revealed a d-d transition envelope similar to that of the wild-type AMT1 protein (Figure 3).

The results are consistent with Cys11, Cys23, and His25 serving as Zn(II) ligands. Since Cys11 exists as a CxxC sequence, the expectation is that Cys14 would be the fourth ligand. To test this prediction, we synthesized 42-residue polypeptides corresponding to residues 1−42 of wild-type AMT1 and ACE1 by solid-state peptide synthesis using Fmoc chemistry. The rationale for the synthesis was to determine whether the 42-residue AMT1 peptide would bind metals with similar properties as intact AMT1 and whether similar coordination properties were exhibited by the ACE1 peptide. Synthetic AMT1−42 and ACE1−42 eluted as

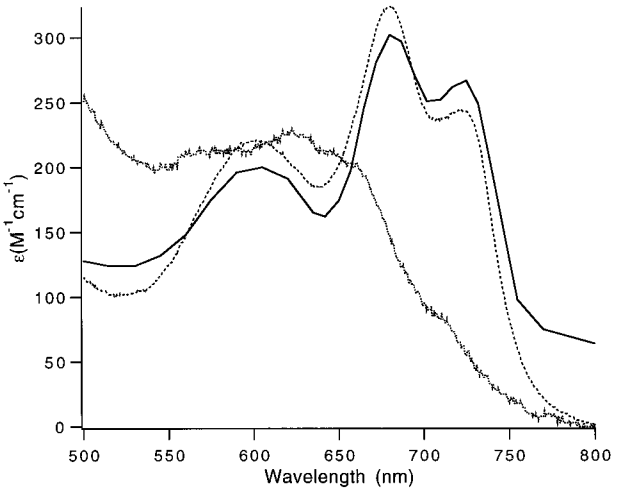

FIGURE 3: Electronic spectra of Co(II) complexes of AMT1 and two AMT1 mutants. The spectrum of Co_1Cu_4AMT1 is shown as the solid line. The sample was prepared by the addition of 1.2 mol equiv of Co(II) to Zn-free Cu_4AMT1. Spectra are shown of the corresponding mutant Co_1Cu_4AMT1 complexes with substitutions at codons 11 (dotted line) and 61 (dashed line).

single peaks off C_{18} reverse-phase HPLC. Electrospray mass spectrometry of the purified peptides revealed masses of 4675.5 amu and 4656.2 amu for AMT1−42 and ACE1−42, respectively. The expected masses of each peptide are 4676.5 and 4657.5, respectively.

The AMT1−42 and ACE1−42 peptides were found to bind a single Zn(II) or Cd(II) ion. Titration of ACE1−42 (Figure 4A) and AMT1−42 (Figure 4B) with increasing quantities of Cd(II) revealed maximal intensity of S→Cd charge transfer transition in the ultraviolet at 1 mol equiv. There was no change in the spectra of each peptide with 2 mol equiv of Cd(II). Reconstitution of each peptide with excess Zn(II) followed by gel filtration resulted in the recovery of the AMT1−42 and ACE1−42 peptides with 1.1 and 0.8 mol equiv of Zn(II) bound, respectively. Titrations of each peptide with Cu(I) stabilized as the Cu−acetonitrile complex and monitoring the samples for luminescence revealed maximal emission in each case with a 1:1 complex of Cu(I) and the peptide (data not shown). Although Cu(I) can bind to the isolated AMT1−42 domain peptide, no Cu(I) binding was observed in this domain as part of the intact AMT1 protein (Thorvaldsen et al., 1994).

Electronic spectroscopy was carried out on Co(II) complexes of AMT1−42 and ACE1−42 (Figure 5). The d-d transition evelope of AMT1−42 was similar to that of wild-type, intact AMT1 in terms of energy of the particular transitions (Figure 5A). A clear 740 nm transition was seen in both CoAMT1−42 and Co,Cu_4AMT1 (compare Figure 3A and 5A). The similar energy profile of the d-d transitions is suggestive of similar coordination environments in both complexes. However, the extinction coefficients of the d-d bands in the CoAMT1−42 peptide complex were higher than those in the intact protein. These extinction differences may arise from an influence of the copper module on the electronic spectra of bound Co(II). The spectrum of the Co(II) complex of ACE1−42 was similar to that of Co-AMT1−42 (Figure 5A). In each Co(II)−peptide complex, two S→Co charge transfer bands were observed at 310 and 334 nm, with extinction coefficients of 2910 and 2788, respectively (Figure 5B). These S→Co charge transfer bands

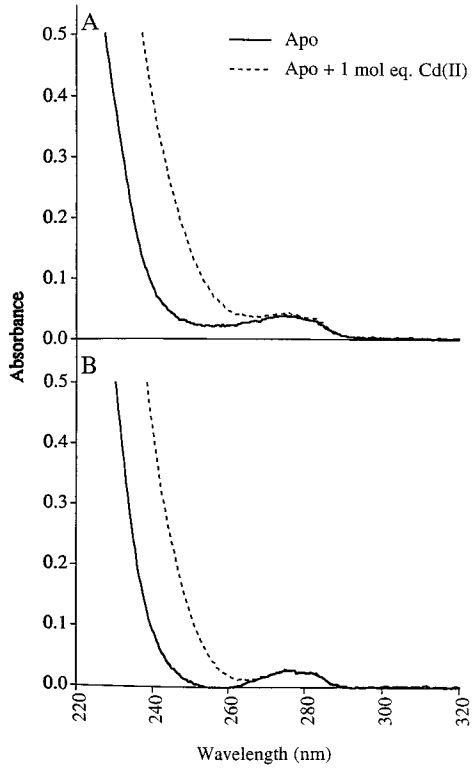

FIGURE 4: Absorption spectra of ACE1-42 (panel A) and AMT1-42 (panel B) peptides in the presence and absence of Cd(II). Apopeptides were mixed with 0, 1, and 2 mol equiv of Cd(II) and neutralized to pH 7.4 prior to recording of the absorption spectra. The spectra of the samples with 2 mol equiv of Cd(II) were superimposable with spectra of samples with 1 mol equiv of Cd-(II).

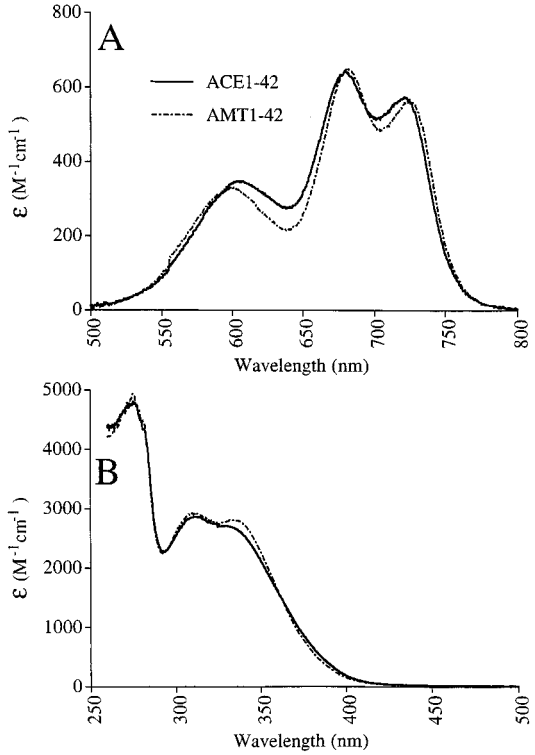

FIGURE 5: Electronic spectra of Co(II) complexes of AMT1−42 and ACE1−42. Peptides (300 nmol) were mixed anaerobically with 1.1 mol equiv of Co(II) and the pH was adjusted to 7.4 with Tris. Panel A shows the d-d envelope in the visible region and panel B is the near UV region where the S→Co charge transfer bands predominate.

are obscured in Co_1,Cu_4AMT1 by S→Cu charge transfer bands.

The mentioned results on H25S mutant AMT1 may imply that either the imidazole of His25 serves as a Zn(II) ligand or it is structurally important in stabilizing the Zn(II) site. The AMT1 sequence in the region of His 25 is C_{23}EHND$_{27}$. If His25 was not a ligand, likely candidates for the fourth ligand are His18 or Asp27. To discriminate between an imidazole or carboxylate as a ligand NMR was carried out on a $^{113}Cd_1$AMT1−42 complex (Figure 6A). A single resonance was observed at 669 ppm, which is within the range expected for Cd(II) coordinated by 4 S-donor ligands or 3 S-donors and a single N-donor (South et al., 1989). ^{113}Cd NMR was attempted of the intact 110-residue AMT1 as a $^{113}Cd_1$,Cu_4AMT1 complex, but no signal was observed under similar conditions. However, the proton spectrum was significantly broader than the proton spectrum of the ^{113}CdAMT1−42 complex, a situation that may have led to ^{113}Cd line broadening in the intact protein.

The identity of the fourth coordinated ligand was determined unambiguously using ^{1}H−^{113}Cd heteronuclear multiple-quantum coherence (HMQC) spectroscopy (Figure 6B). In the HMQC experiment the only signals observed are those protons that are scalar coupled to ^{113}Cd. Correlation signals were observed in the aliphatic regions consistent with Cys(β) protons. In addition, correlation signals were observed for the two His ring protons (7.3 ppm for H^2 and 7.1 ppm for H^4). This provided clear indication that a His imidazole is coordinated to ^{113}Cd(II). As the H^2 imidazole signal is of greater intensity than the H^4 signal, the ^{113}Cd coordination may occur at the Nδ atom lone electron pair. From this information we cannot discern whether His18 or His25 provides the coordinating nitrogen.

The results are suggestive that ACE1 and AMT1 consist of an N-terminal Zn(II) module followed by a tetracopper module. The existence of Zn(II) in ACE1 and AMT1 is based largely on work with bacterially expressed proteins. To address whether ACE1 contains a bound Zn(II) in Cu-treated yeast, we attempted to purify ACE1 from yeast after overexpression of an affinity-tagged ACE1 molecule. We were unsuccessful in obtaining adequate quantities for physical measurements. A second strategy to demonstrate that the N-terminal module in Cu-activated ACE1 contains a bound Zn(II) was to mutagenize the entire *ACE1* gene to create Cys→Asp substitutions at codons 11 and 23. The carboxylate of aspartate is a common Zn(II) ligand, whereas it would be an unfavorable Cu(I) ligand. Thus, the rationale of our strategy is that if a particular cysteine is a Zn(II) ligand, then a Cys→Asp substitution may retain function whereas Cys→Ser or Cys→Tyr substitutions would inactive ACE1. In contrast, if a particular Cys was a Cu(I) ligand, a Cys→Asp substitution would be expected to be equivalent to a Cys→Ser substitution and result in a nonfunctional molecule. It is already known that Cys11 and Cys23 are critical for *in vivo* function of ACE1 (Hu et al., 1990). Substitution resulting in Cys11→Tyr or Cys11→Ser and Cys23→Ser inactivate ACE1 (Hu et al., 1990).

We engineered Cys→Asp substitutions at codons 12 and 23 as well as the nonfunctional Cys→Tyr and Cys→Ser substitutions at codons 11 and 23, respectively. The mutant ACE1 molecules were tested in DTY23 yeast cells which harbors a nonfunctional ACE1 (the *ace1-1* mutation in

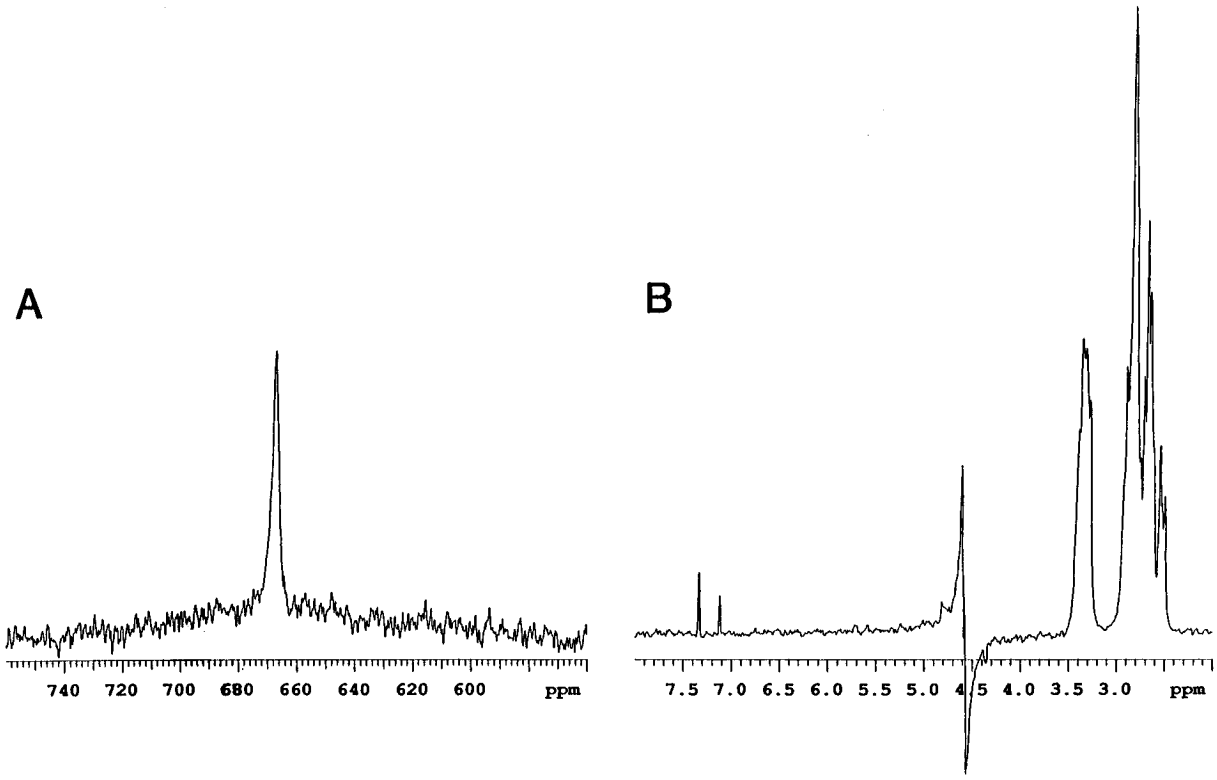

FIGURE 6: ^{113}Cd and heteronuclear multiple quantum coherence NMR of Cd_1AMT1−42. The AMT1−42 peptide (3.2 mg) was mixed with 1 mol equiv. ^{113}Cd(II) and neutralized to pH 7. The sample was concentrated by ultrafiltration on an Amicon YC 05 membrane. For the ^{113}Cd readout in panel A the chemical shift is relative to 1 M $Cd(ClO_4)_2$. The number of transients was 57 000. Samples contained ^2H_2O as a field lock. Parameters used included a spectral width of 22.2 kHz, an acquisition time of 0.8 s, and a pulse width of 60°. A 40 Hz line broadening was applied for spectral enhancement. Heteronuclear multiple-quantum coherence NMR of $^{113}Cd_1$AMT1−42 is shown in panel B. The one-dimensional $^1H-^{113}Cd$ multiple quantum filtered proton NMR spectrum was acquired using a standard HMQC pulse sequence (Bax et al., 1986). The 1/(2J) delay was set at 8.3 ms. The H2 and H4 ring protons of His appear at 7.3 and 7.1 ppm, respectively.

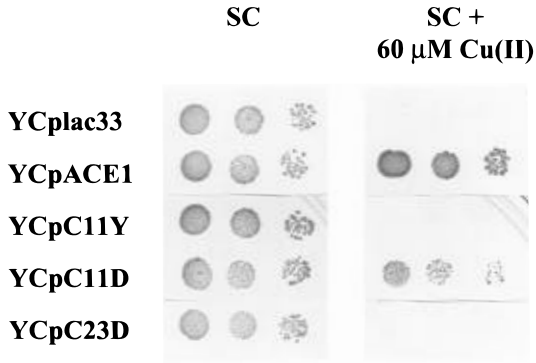

FIGURE 7: Copper tolerance of *ACE1* mutants. *ACE1* with mutations at codons 11 or 23 were expressed in DTY23 yeast cells lacking a functional ACE1. The mutant genes were present on a centromere-based plasmid and cells harboring the mutants listed or the control plasmid (YCplac33) were plated on synthetic complete medium in the presence or absence of 60 μM $CuSO_4$.

DTY23 is Cys11→Tyr). A functional ACE1 is essential for the expression of *CUP1* encoding metallothionein. The expression of metallothionein allows cells to propagate in medium containing copper salts.

Cells harboring the wild-type *ACE1* gene on a YCp vector were able to grow in medium containing 60 μM Cu(II), whereas transformants containing the control plasmid YCplac33 were growth arrested (Figure 7). As expected, the Cys11Tyr substitution in *ACE1* failed to support growth of cells in Cu-containing medium. The Cys11Asp substitution did result in a partially functional ACE1 molecule in that cells were capable of limited growth in medium containing 60 μM $CuSO_4$. Cells harboring the Cys11Asp mutation were compromised in growth relative to cells with the wild-type ACE1, yet the limited growth is consistent with Cys11 being a Zn(II) ligand *in vivo*. This result provides *in vivo* support for the N-terminal domain of ACE1 and, therefore, AMT1 serving as a conserved Zn(II) module. The Cys23Asp substitution failed to support growth of DTY23 cells as is the case of the Cys23Ser mutation. The lack of growth with Asp at codon 23 must indicate the essential nature of cysteine at that sequence position.

DISCUSSION

Previous studies demonstrated that the N-terminal half of the ACE1 and AMT1 polypeptides form specific DNA complexes in a Cu-dependent fashion (Furst et al., 1988; Buchman et al., 1989; Thorvaldsen et al., 1994). We demonstrated that the 110-residue N-terminal fragment of AMT1 bound 4 Cu(I) ions and a single Zn(II) ion (Thorvaldsen et al., 1994). The single Zn(II) ion is shown here to be coordinated within the N-terminal 42 residues in AMT1. The 122-residue N-terminal fragment of ACE1 also exists as a Cu_4Zn_1ACE1 complex. Since ACE1 and AMT1 exhibit 64% sequence identity in their N-terminal sequences, we expect ACE1 to exhibit a N-terminal Zn site. The prediction is then that AMT1 and ACE1 consist of two contiguous modules, residues 1−42 forming an independent Zn(II) module and residues 43−110 enfolding a tetracopper cluster. The basis for this conclusion that the Zn(II) site is localized within N-terminal 42 residues of each protein is summarized below.

The first prediction was that mutations within Zn(II) ligand codons would not alter the DNA binding activity of AMT1.

We previously demonstrated that Zn-free AMT1 bound its cognate DNA site with nearly equal affinity as the Cu_4Zn_1-AMT1 complex (Thorvaldsen et al., 1994). Therefore, mutations in AMT1 that reduced Zn(II) affinity would be predicted to bind DNA, whereas mutations that disrupted the Cu(I) cluster may be expected to compromise DNA binding activity. Mutations of C11, C23, and H25 codons of AMT1 did not reduce binding, whereas the other four mutations attenuated DNA binding.

The second prediction was that Zn ligand mutations should reduce the bound Zn content or create a more labile Zn site. This was observed with C11Y, C23S, and H25S mutants. The C11Y mutant protein bound 1 mol equiv of Zn(II), but occupancy of the Zn site in the mutant protein was eliminated by electrospray ionization. Zn(II) populates the site in the wild-type protein after ionization suggesting that the C11Y mutation reduced Zn(II) site affinity. The single Zn(II) in the C11Y mutant may be stabilized by the adjacent aspartyl residue or perhaps the tyrosyl residue itself may provide a liganding oxygen. It is clear that metal binding in mutant AMT1 molecules is complex. For example, the His25Ser AMT1 had a reduced Zn(II) content but elevated copper content. Likewise, the Cys90Ser mutant AMT1 had elevated levels of bound Zn(II).

The third line of evidence that the N-terminal segment of AMT1 formed the Zn(II) site was that substitution of Co(II) for the bound Zn(II) ion in the C11Y mutant AMT1, but not the C61S mutant AMT1 molecule, blue-shifted the envelope of d-d transitions seen in the wild-type Cu_4Co_1-AMT1 complex. The C11Y substitution would be expected to blue-shift the d-d transitions envelope if the Cys11 thiolate was a ligand and if the substitution removed a thiolate ligand.

The evidence supports a model of AMT1 and ACE1 in which the N-terminal 42 residues enfolds a Zn(II) site and residues 43−110 form the tetracopper center. It is likely that the N-terminal domain is occupied by Zn(II) in Cu-activated yeast based on the partial function of the Cys11Asp mutant ACE1.

To confirm that the N-terminal segment of ACE1 and AMT1 existed as a conserved Zn module, we showed that whereas a Cys11Tyr or Cys11Ser mutation abolished *in vivo* function of ACE1, a Cys11Asp substitution maintained partial function of the ACE1 transcription factor. A Cys11Asp substitution would be expected to be a nonfunctional substitution if Cys11 was a Cu(I) ligand but may be permissible as a Zn(II) ligand. This result is suggestive that Cu-activated ACE1 contains a bound Zn(II) ion within the N-terminal module.

It appears that the N-terminal 42 residues in AMT1 form an independently folded module as the synthetic 42-mer formed a Co(II) complex with electronic properties similar to those of the intact 110-mer. The corresponding peptide from ACE1, likewise, forms a stable Zn(II) complex. The Zn(II) complex of the AMT1−42 peptide appears folded on the basis of circular dichroism, but prediction of secondary structure is not feasible as significant differences are observed in ellipticities of Zn(II) and Cd(II) complexes of AMT1−42 (data not shown). Although the differences may arise from structural differences, it is more likely that differences arise from chirality of the metal centers.

The Zn module in AMT1 appears to be an independently folded domain. The presence of the C_{11}-X-X-C_{14} motif as with other Zn-binding CxxC sequence motifs may fold into a "rubredoxin knuckle" with NH−S hydrogen bonding of backbone amide protons and sulfur atoms (Blake & Summer, 1994). These NH−S hydrogen bonds appear to stabilize a tight turn conformation. The presence of Zn(II) in an independently folded domain may explain the lack of observed Cu−Zn backscattering in Zn EXAFS.[1]

The single Zn(II) ion within the conserved Zn structural module exhibits S_3N_1 coordination. There are two conserved histidyl residues in the N-terminal segments of AMT1 and ACE1, i.e., His18 and His25. His25 may be the candidate Zn ligand as Zn module proteins typically contain coordinating ligands separated by 2−3 intervening residues. If His18 were the fourth ligand there would be a four residue spacing between His18 and Cys23. We predict that conserved Zn module will be a CCCH module with ligand spacing of C-X_2-C-X_8-C-X-H. Multidimensional NMR in progress will provide unambiguous verification whether His18 or His25 is the liganding imidazole.

The first 42 residues of ACE1 and AMT1 are homologous to two other transcription factors in *S. cerevisiae*, MAC1 (Jungmann et al., 1993) and a 694-residue ACE1-like ORF identified from the yeast sequencing project (Figure 8). Homologous molecules are also found in *Yarrowia lipolytica* and *Schizosaccharomyces pombe* (Figure 8). The other homologue for which functional information is available is MAC1. MAC1 is required for basal expression of *FRE1* and *CTR1* (Jungmann et al., 1993; Hassett & Kosman, 1995). The implication of the sequence homology is that MAC1, like ACE1 and AMT1, will contain an N-terminal, conserved Zn module. We have shown that the Lpz8p ORF from *S. cerevisiae* is an expressed gene and are currently investigating its *in vivo* function.

The sequence similarity between ACE1 and the other five molecules shown in Figure 8 is most pronounced within the N-terminal 40 residues. The homology between ACE1, MAC1, and the *S. pombe* ORF (AC31a2) is confined to only the N-terminal 40 residues. The sequence homologies do not aid in addressing which histidine is the fourth Zn(II) ligand as both His18 and His23 are conserved in the six sequences (Figure 8).

If AMT1 and ACE1 contain a conserved Zn module, the question arises as to the function of the module in these transcription factors. ACE1 appears to be distinct from AMT1 in one regard. Whereas mutations in the Zn module of AMT1 do not dramatically alter DNA binding, mutations in the corresponding codons in ACE1 do affect DNA binding. The original *ace1-1* mutant protein contained a C11Y substitution, and DNA binding affinity was reduced nearly 10-fold (Buchman et al., 1990). CuACE1 modified with iodoacetate in which Cys11, Cys14, and Cys23 were >90% alkylated showed impaired DNA binding by 10-fold compared to unmodified CuACE1 (Dobi et al., 1995). Although the *in vitro* DNA binding affinity was reduced nearly 10-fold, the *in vivo* function of *ace1-1* was abolished (Thiele, 1988; Buchman et al., 1990). Likewise, ACE1 lacked *in vivo* function when Cys→Ser substitutions were present at any position other than Cys105, which is not a conserved cysteinyl residue between ACE1 and AMT1 (Hu et al., 1990).

[1] G. N. George, R. A. Farrell, and D. R. Winge, unpublished observation.

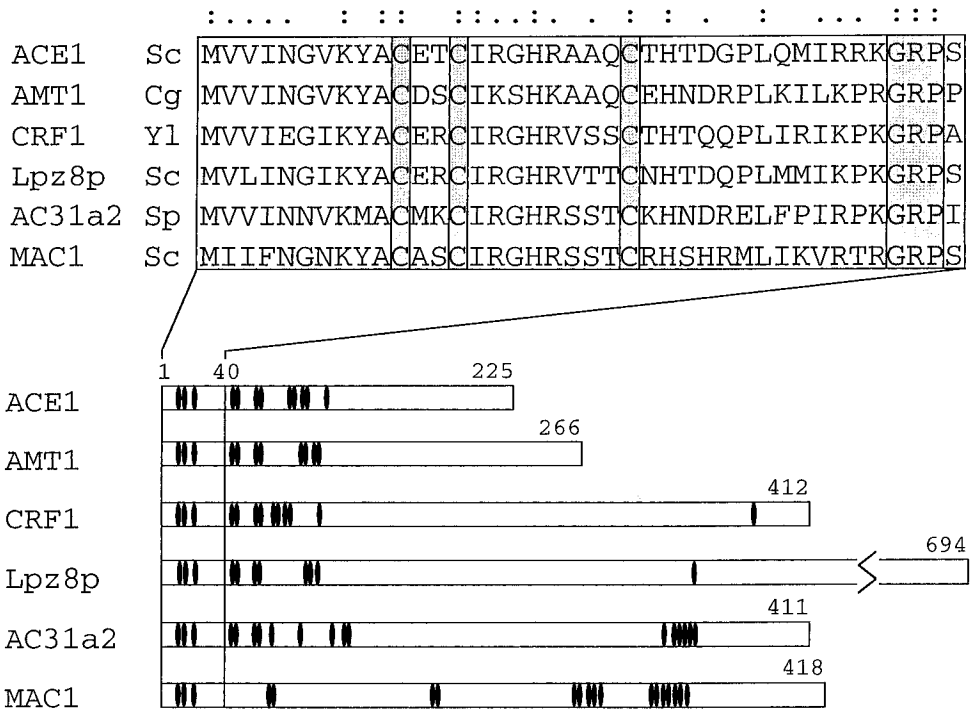

FIGURE 8: Sequence conservation of the Zn module in distinct molecules. The sequences of the Zn module of ACE1 and AMT1 are aligned with the corresponding sequences of MAC1 and three homologs identified in DNA sequencing projects. CRF1 is the ACE1-like molecule from *Yarrowia lipolytica*, Lpz8z is the designation of a ACE1-like ORF from chromosome 16 of *S. cerevisiae*, and AC31a2 is a MAC1-like ORF from *S. pombe*. The filled ovals designate positions of cysteinyl residues.

Footprint analysis of the mutant *ace1-1* protein and the aklyated CuACE1 complex revealed a restricted set of protein−DNA contacts (Buchman et al., 1990; Dobi et al., 1995). In each case, the protein protected only half the UAS site from methylation interference, and in the case of *ace1-1* 10-fold more protein compared to wild-type CuACE1 was required for complete protection of the restricted site (Buchman et al., 1990). The base-specific contacts in the distal segment of the ACE1 binding site were abolished with the mutant or modified proteins (Buchman et al., 1990; Dobi et al., 1995). The minimal ACE1 binding site on the *CUP1* UAS_c was shown to be 5′ *GCG*TCTTTTCGCTGA 3′ with the 5′ italic region designated as the distal segment (Dobi et al., 1995). Relatively weak interactions occur in the distal segment compared to the strong interactions observed in the A/T-rich central segment and proximal region containing the conserved GCTG core sequence (Dobi et al., 1995). The Zn module in ACE1 is likely responsible for the major groove contacts in the distal segment of the UAS_c. However, the Zn module itself present as the ACE1−42 peptide in either a Zn(II) or Cu(I) complex failed to form a specific DNA complex with the *CUP1* UAS_c DNA duplex (data not shown).

Whereas the Zn module in ACE1 makes specific DNA base contacts, any contribution of the Zn module in AMT1 to DNA binding is less obvious (Thorvaldsen et al., 1995). The DNA binding sites of AMT1 contain the same A/T-rich segment and conserved proximal GCTG sequence, but no homology exists in the distal GCG sequence in which major groove ACE1 contacts occur (Zhou et al., 1992). The preliminary mapping studies of the AMT1 DNA binding site revealed base-specific contacts in the A/T-rich region and in the proximal GCTG region (Zhou et al., 1992). It is conceivable that the Zn module in AMT1 makes only limited phosphate backbone contacts on the DNA, or alternatively the Zn module in AMT1 may not function in DNA binding unlike the situation in ACE1.

The Zn module may have multiple functions. In ACE1 DNA binding appears to be important. In ACE1 and AMT1, the Zn module may also have a structural role. The contacts of ACE1 with the A/T-rich central segment occur within a minor groove (Dobi et al., 1995). Although the segments of ACE1 and AMT1 responsible for minor groove interactions are not known, both proteins contain a sequence adjacent to the Zn(II) module (RGRP residues 36−39) that is homologous to a DNA minor groove binding motif found in high mobility group (HMG) proteins (Geierstanger et al., 1994; Johnson et al., 1989). The Zn modules in ACE1 and AMT1 may be important in stabilizing a particular conformation of that HMG-like sequence. Adjacent to the conserved Zn module in MAC1 is the same RGRP sequence found in ACE1 and AMT1. Since MAC1 is a known basal transcription factor, these two structural regions in MAC1 may function in DNA binding as in ACE1. The conservation of the Zn module in six molecules spanning four distinct yeast strains suggests that the module may have a common function.

ACKNOWLEDGMENT

We thank Dr. R. Schackmann for carrying out the Fmoc synthesis of the 42 mer AMT1 peptide, Jay I. Olsen for technical NMR assistance, and Dr. J. McCloskey for mass spectrometry. We acknowledge support from the National Institutes of Health (5P30-CA 42014) to the Biotechnology Core Facility for DNA synthesis and solid phase peptide synthesis. Support is also acknowledged to the Utah Regional Cancer Center Grant 5P30 CA 42401 for support of the Electrospray Mass Spectrometry Core Facility.

REFERENCES

Bax, A., & Subramanian, S. (1986) *J. Magn. Reson. 67*, 565−569.

Bax, A., Griffey, R. H., & Hawkins, B. L. (1983) *J. Magn. Reson. 55*, 3012−3015.

Blake, P. R., & Summers, M. F. (1994) *Adv. Inorg. Biochem. 10*, 201−228.

Bradford, M. M. (1976) *Anal. Biochem. 72*, 248−254.

Buchman, C., Skroch, P., Dixon, W., Tullius, T. D., & Karin, M. (1990) *Mol. Cell Biol. 10*, 4778−4787.

Buchman, C., Skroch, P., Welch, J., Fogel, S., & Karin, M. (1989) *Mol. Cell. Biol. 9*, 4091−4095.

Dameron, C. T., Winge, D. R., George, G. N., Sansone, M., Hu, S., & Hamer, D. (1991) *Proc. Natl. Acad. Sci. U.S.A. 88*, 6127−6131.

Dance, I. G. (1986) *Polyhedron 5*, 1037−1104.

Dance, I. G. (1978) *Aust. J. Chem. 31*, 2195−2206.

Dobi, A., Dameron, C. T., Hu, S., Hamer, D., & Winge, D. R. (1995) *J. Biol. Chem. 270*, 10171−10178.

Ecker, D. J., Butt, T. R., Sternberg, E. J., Neeper, M. P., Debouck, C., Gorman, J. A., & Crooke, S. T. (1986) *J. Biol. Chem. 261*, 16895−16900.

Fogel, S., & Welch, J. W. (1982) *Proc. Natl. Acad. Sci. U.S.A. 79*, 5342−5346.

Fogel, S., Welch, J. W., Cathala, G., & Karin, M. (1983) *Current Genet. 7*, 347−355.

Furst, P., Hu, S., Hackett, R., & Hamer, D. (1988) *Cell 55*, 705−717.

Geierstanger, B. H., Volkman, B. F., Kremer, W., & Wemmer, D. E. (1994) *Biochemistry 33*, 5347−5355.

Hamer, D. H. (1986) *Annu. Rev. Biochem. 55*, 913−951.

Hamer, D. H., Thiele, D. J., & Lemontt, J. E. (1985) *Science 228*, 685−690.

Hassett, R., & Kosman, D. J. (1995) *J. Biol. Chem. 270*, 128−134.

Hu, S., Furst, P., & Hamer, D. (1990) *New Biol. 2*, 544−555.

Johnson, K., Lehn, D., & Reeves, R. (1989) *Mol. Cell. Biol. 9*, 2114−2123.

Jungmann, J., Reins, H.-A., Le, J., Romeo, A., Hassett, R., Kosman, D., & Jentsch, S. (1993) *EMBO J. 12*, 5051−5056.

Karin, M., Najarian, R., Haslinger, A., Valenzuela, P., Welch, J., & Fogel, S. (1984) *Proc. Natl. Acad. Sci. U.S.A. 81*, 337−341.

Mehra, R. K., Garey, J. R., & Winge, D. R. (1990) *J. Biol. Chem. 265*, 6369−6375.

Mehra, R. K., Thorvaldsen, J. L., Macreadie, I. G., & Winge, D. R. (1992) *Gene 114*, 75−80.

Nakagawa, K. H., Inouye, C., Hedman, B., Karin, M., Tullius, T. D., & Hodgson, K. O. (1991) *J. Am. Chem. Soc. 113*, 3621−3623.

Narula, S. S., Mehra, R. K., Winge, D. R., & Armitage, I. M. (1991) *J. Am. Chem. Soc. 113*, 9354−9358.

Palmiter, R. D. (1987) *Experentia Suppl. 52*, 63−80.

Pickering, I. J., George, G. N., Dameron, C. T., Kurz, B., Winge, D. R., & Dance, I. E. (1993) *J. Am. Chem. Soc. 115*, 9498−9505.

Robbins, A. H., McRee, D. E., Williamson, M., Collett, S. A., Xuong, N. H., Furey, W. F., Wang, B. C., & Stout, C. D. (1991) *J. Mol. Biol. 221*, 1269−1293.

Sewell, A. K., Jensen, L. T., Erickson, J. C., Palmiter, R. D., & Winge, D. R. (1995) *Biochemistry 34*, 4740−4747.

South, T. L., Kim, B., & Summer, M. J. (1989) *J. Am. Chem. Soc. 111*, 3395−3396.

Thiele, D. J. (1988) *Mol. Cell Biol. 8*, 2745−2752.

Thiele, D. J., & Hamer, D. H. (1986) *Mol. Cell Biol. 6*, 1158−1163.

Thorvaldsen, J. L., Sewell, A. K., McGowen, C. L., & Winge, D. R. (1993) *J. Biol. Chem. 268*, 12512−12518.

Thorvaldsen, J. L., Sewell, A. K., Tanner, A. M., Peltier, J. M., Pickering, I. J., George, G. N., & Winge, D. R. (1994) *Biochemistry 33*, 9566−9577.

Welch, J., Fogel, S., Buchman, C., & Karin, M. (1989) *EMBO J. 8*, 255−260.

Zhou, P., & Thiele, D. J. (1991) *Proc. Natl. Acad. Sci. U.S.A. 88*, 6112−6116.

Zhou, P., Szczypka, M. S., Sosinowski, T., & Thiele, D. J. (1992) *Mol. Cell. Biol. 12*, 3766−3775.

BI9517087